Insulinotropic effect of *Teucrium polium*; Identification of potential mechanistic drug targets

Adnan Mannan, Erik Helmerhorst, Rodrigo Carlessi and Rima Caccetta*

Curtin Medical School, Curtin Health Innovation Research Institute, Faculty of Health Sciences, Curtin University, Perth, Western Australia, Australia.

ABSTRACT

Teucrium polium (*T. polium*)*,* commonly known as golden germander, is a herb that grows in the Mediterranean region and is used by the locals to treat *diabetes mellitus*. The glucose-lowering effect of *T. polium* is well established in rodents. This study aims to examine whether the glucose-lowering effect is by inducing the release of insulin from pancreatic beta cells and to identify key measurable biomolecules/sites that are modified in the lead-up to insulin release. Insulin secretion was examined in BRIN-BD11 pancreatic beta cells treated with *T. polium* extract *in vitro* and key flavonoids were identified using LCMS. The *T. polium* extract promoted increased insulin secretion ($p<0.05$), in a dose-dependent manner, and increased glucose uptake ($p<0.05$) within 30min. This was accompanied by an increase in GLUT2 ($p<0.05$) and glucokinase ($p<0.01$) expression. Also, mitochondrial metabolism and glycolytic rates were enhanced ($p<0.05$), and ATP production increased ($p<0.01$), which coincided with increased ($p<0.01$) calcium influx. Rutin and apigenin were detected, but not quercetin, in this extract. *T. polium* promotes insulin secretion. *T. polium* does this by GLUT2 and glucokinase expression, increased glucose transport, metabolism and ATP production, ultimately increasing intracellular calcium.

Keywords: Diabetes mellitus, phenolics, flavonoids, hyperglycaemia, glucose lowering, insulin secretagogue, pancreatic beta cells.

*Corresponding author. E-mail: r.caccetta@curtin.edu.au.

INTRODUCTION

Diabetes mellitus (DM) is a metabolic disorder that is increasing at an alarming rate and is recognised as the fastest growing chronic disease in the world (Dagenais et al., 2016; Menke et al., 2016; WHO, 2006). It is characterised by hyperglycaemia, mostly resulting from defects in insulin secretion, insulin action, or both (Del Prato et al., 1993; Leahy et al., 1992; Rossetti et al., 1987).

Glucose is the primary stimulus for insulin secretion in human and rodent beta cells (Ashcroft et al., 1984; Rutter et al., 2015). The amount of insulin secreted in the presence of glucose exceeds that in the presence of either fat or protein. Increased transport of glucose into beta cells via GLUT2 and commitment of glucose to glycolysis by the action of glucokinase potentiates insulin secretion through an increased ATP/ADP ratio as well as by generation of other coupling factors during oxidative

phosphorylation (Fu et al., 2013). GLUT2 is the first glucose sensor in the beta cell that equilibrates glucose by facilitated diffusion which occurs rapidly. Thereafter, glucokinase responds to rises in blood glucose levels by phosphorylating glucose to produce glucose-6-phosphate. This reaction is the rate-limiting step in glycolysis and thus acts to commit glucose to glycolysis (Ferre et al., 1996; German, 1993; Matschinsky, 1990). The formation of pyruvate is the endpoint of glycolysis, where it is further metabolised by the tricarboxylic acid cycle in the mitochondria of beta cells to produce ATP (Suckale and Solimena, 2008). As a result of higher ATP production, the intracellular ATP/ADP ratio is increased. This further facilitates the closure of ATP-sensitive potassium (K_{ATP}) channels (Maechler and Wollheim, 2000; Markworth et al., 2000). This depolarizes the plasma membrane and opens the voltage-gated calcium

channel, thereby facilitating calcium entry into beta cells (Maechler and Wollheim, 1999; Maechler and Wollheim, 2000). This activates the exocytosis of insulin from insulin secretory granules as they move towards the plasma membrane (Fu et al., 2013).

Teucrium polium (*T. polium*), had been reported to have various medicinal properties including antibacterial, anti-inflammatory, antioxidant and anti-diabetic effects (Albadr et al., 2022; Abdollahi et al., 2003; Ardestani et al., 2008; Baali et al., 2016; Capasso et al., 1983). Several studies have investigated the glucose-lowering potential of total extracts of *T. polium in vitro*, *ex vivo* and *in vivo* (Esmaeili and Yazdanparast, 2004; Kasabri et al., 2012; Shahraki et al., 2007; Stefkov et al., 2011). There have been other studies that investigated purchased or isolated pure compounds, isomers of which have also been putatively identified in *T. polium*. However, the compound(s) that deliver the glucose-lowering effects of the total extract is yet to be elucidated (Cozzani et al., 2005; Sharififar et al., 2009). Most of the research investigating the glucose-lowering effects of *T. polium* has focused on changes in blood glucose levels and insulin secretion but there is limited information on the pathway leading to that glucose-lowering effect. Identification of the pathway/s will aid in the ultimate isolation of the active constituent/s. This study aimed to investigate: i) whether treatment with the *T. polium* extract promotes insulin secretion from pancreatic beta cells and ii) determine whether the various commonly known signalling molecules are involved in this process when the cells are treated with *T. polium*.

MATERIALS AND METHODS

Plant collection and extraction

The aerial parts of *T. polium L (Labiatae)* were purchased from a herbalist who collected the plant from the Al-Salt region (25km west of Amman), Jordan. The plant was further authenticated by the late Professor Dawud Al-Eisawi, of the Biological Sciences Department, University of Jordan before it was brought into Australia under quarantine: AQIS permit 200515757. The leafy parts of the plant material were freeze-dried.

The *T. polium* extract was prepared as outlined by Ireng et al. (2016). Five grams of the freeze-dried *T. polium* was placed in a Soxhlet apparatus (Electromantle®- EM1000/CE) and refluxed three times (4h) at 80-100°C in 400mL of 90% methanol. The extract was then allowed to cool and the residual non-plant material in the thimble was discarded. The extract was then concentrated in a rotary evaporator (Büchi Rotavapor R-200) at a fixed temperature of 45(±2)°C for 30-40min. The concentrated plant extract was then made up to a 200-mL volume with 90% methanol. Then 2mL aliquots were pipetted into separate glass vials (light protective) and dried under vacuum at room temperature.

Thereafter, the vials were immediately purged under nitrogen (supplied by Comet TM CIGWELD), sealed and stored at -20°C. Each vial contained extract derived from a 50mg equivalent of original plant material. Throughout this paper, the amount of *T. polium* is expressed as the extract obtained from a weight of original plant material. Where this extract is used in culture/buffer, the amount is then stated as an extract obtained from an original weight of plant material per mL of culture medium.

The concentration of the *T. polium* extract used was in line with other studies examining extracts in cell culture. It was selected to be the least possible concentration that is less than 1mg/mL (non-significantly affecting cell viability) which also allowed for a detectable change from control to occur.

Chemical profiling by LCMS

Chemical fingerprint profiling of the plant extract was carried out by Mr Ben Hunter, Curtin Health Innovation Research Institute. Total ion chromatograms (TIC) were collected using a Liquid Chromatography-Mass Spectrometry (LCMS) system: Agilent 6540 UHD Q-TOF MS system (Santa Clara, CA, USA) with a dual sprayer electrospray ionization (ESI) source and attached to an Agilent 1290 infinity UHPLC system (Santa Clara, CA, USA) comprised of a vacuum degasser, binary pump, with a thermostated auto-sampler and column compartment. The MS was operated using the following conditions: nebuliser pressure 35 psi, dry gas flow rate 8L/min, sheath gas temperature 300°C, sheath gas flow rate 11L/min, capillary voltage 3500 V and capillary voltage 500V.

The instrument was operated in the scan mode with data collected in the m/z range of 100 to 1000amu. A Grace c18 monomeric 100*2.1mm, 5µm, 300Å column was used with a flow rate of 200µL/min, maintained at 40 ± 1°C, with a 10.2min run time. A gradient LC method was used with mobile phases comprised of (A) 0.1% formic acid in deionized water and (B) 0.1% formic acid in acetonitrile. Gradient: 6min linear gradient from 5% solvent (B) to 40% solvent (B), followed by a 0.1min linear gradient to 100% solvent (B), then a 2min hold at 100% solvent (B) and a 0.1min return to re-equilibration at 5% solvent (B) holding for 2min. Compounds were identified by HPLC–ESI(+)–QTOF– MS. The identification of apigenin, rutin and quercetin in the *T. polium* extract was carried out using a comparison of accurate mass and retention time of purified commercial standards (apigenin, quercetin dihydrate and rutin hydrate purchased from Sigma) to the *T. polium* extract by generated extracted ion chromatogram (EIC).

Cell culture

The experiments were carried out using the rat

pancreatic beta cell line BRIN-BD11, donated by Professor Philip Newsholme, Curtin University. In brief, BRIN-BD11 cells (passage number 25-30) were grown overnight in Roswell Park Memorial Institute (RPMI) medium (HyClone™ RPMI 1640 media, SH30027.01, GE Healthcare Life Sciences) supplemented with 10% (v/v) fetal bovine serum (FBS) (SerANA (WA) Pty Ltd, Bunbury, Australia), 100Units/mL penicillin and 0.1mg/mL streptomycin (Hyclone penicillin-streptomycin 100X solution, Thermo Fisher Scientific), maintained in 5% CO_2 in a NUAIRE automatic CO_2 incubator at 37°C.

Cell viability assays

Briefly, 5000 BRIN-BD11 cells per well were seeded in a 96-well plate. The medium was discarded on the next day and cells were treated with different doses of *T. polium* extract in growth medium for 24h. The MTT tetrazolium assay was carried out as described by Kauffman et al., 2012; absorbance was monitored at 550nm. The Acid phosphatase assay was carried out as described by Friedrich et al. (2007) and Patel et al. (2016), absorbance was monitored at 405nm. Data was recorded using a plate reader (EnSpire® Multimode plate reader, Perkin Elmer).

Insulin secretion

BRIN-BD11 cells were grown in 24-well plates at 1.5 x 10^5 cells/well in 1mL of medium. Medium was discarded after 24h followed by washing twice with PBS (Hyclone phosphate buffered saline, In Vitro Technologies). All the treatments were incubated in Krebs Ringer bicarbonate (KRB) buffer following the method of Chen et al. (2016). The glucose concentration was determined based on previous studies (McClenaghan et al., 1996). Insulin release was measured using the Mercodia Rat Ultrasensitive Insulin ELISA kit (Mercodia, Uppsala, Sweden). The absorbance of samples was measured at 450 nm using a plate reader. Sample readings were normalized by measuring the protein concentration using Pierce BCA (bicinchoninic acid) Protein Assay Kit.

Glucose uptake

Glucose uptake was measured using a flow cytometry-based method, similar to Carlessi et al., 2017. Briefly, serum-starved (6h) BRIN-BD11 cells were treated for 30min with the *T. polium* extract (50 or 500µg/mL) or with DMEM media (Gibco- DMEM (high glucose, GlutaMAX(TM), pyruvate). The fluorescently labelled glucose analogue 2- [*N*-(7-nitrobenz-2-oxa-1, 3-diazol-4-yl) amino]-2-deoxy-d-glucose (2NBDG) (Thermo Fisher Scientific, San Jose, CA, USA) was utilized as an indicator to estimate glucose uptake. The glucose uptake by cells was quantified by measuring the shift in median fluorescence compared to control unlabelled cells after suitable gating strategies were implemented to eliminate cell debris, doublets and dead cells. For each measurement, ten thousand single-cell events were recorded. Measurements were done using a FACS LSR Fortessa flow cytometer (BD Biosciences, Heidelberg, Germany). FlowLogic FCS analysis software (Inivai Technologies, Melbourne, Australia) was used to analyse the data.

Western Blot

BRIN-BD11 cells were cultured and then glucose starved for 40min in KRB buffer containing 1.1 mM glucose. Cells were then treated for 30min with control glucose (5.5mM), or *T. polium* extract (500µg/mL in 5.5mM glucose). Cell lysates were collected and used for Western Blot. The cells were lysed for 40min on ice using the radioimmunoprecipitation assay buffer (supplemented with Pierce™ protease inhibitor mini tablets). Equal amounts of protein (40 µg) were separated by SDS-PAGE, using 10% separating gels, and then the samples were transferred to polyvinylidene fluoride membranes. The membranes were blocked with 3% bovine serum albumin in 0.05% Tris-buffered saline with Tween 20 (TBST) solution and incubated overnight at 4°C with the primary antibody. Anti-glucokinase antibody-N-terminal (Abcam, ab37796) and Anti-Glucose Transporter GLUT2 antibody (Abcam, ab54460) were investigated in the study. Primary antibodies were used at 1:200-fold dilutions from stock concentrations. After washing with 1% (w/v) TBST three times, the membranes were incubated for 1h (at room temperature) with horseradish peroxidase-conjugated goat anti-rabbit IgG (Agilent's Dako, Glostrup, Denmark), at a ratio of 1:40000 in blocking buffer. The membranes were then washed three times with 1% (w/v) TBST and the immunoreactive bands were visualized using ECL detection reagents. Images were captured using Molecular Imager® Gel Doc™ XR System (BIO-RAD, USA). Densitometric analysis was done by using the BIO-RAD Image Lab Software (version 5.2.1). Clarity™ Western ECL Substrate, protein ladder (Precision plus protein ® standard) and tetramethylethylenediamine (TEMED) were purchased from BIO-RAD Laboratories Pty. Ltd., Life Science (Gladesville, NSW, Australia).

Immunofluorescence microscopy for GLUT2 expression analysis

BRIN-BD11 cells were grown in 6-well plates. Cells were serum starved for 6h and immediately treated for 24h with *T. polium* extract. The cells were then prepared for

immunofluorescence microscopy according to the method of Chaturvedi et al. (2015). Cells were glucose starved for 40min in KRB buffer containing 1.1mM glucose. Cells were then treated for 30min with 5.5 mM glucose (control) or *T. polium* extract (500µg/mL in 5.5mM glucose) in KRB buffer. Cells were stained with antibodies and observed in an Olympus upright microscope to obtain images of GLUT2 and DAPI (Sigma- Aldrich) nuclear staining. The fluorescence intensity of GLUT2 observed in BRIN-BD11 cells was measured using ImageJ ® software (Ver. 1.50i). Analysis of fluorescence intensity and detection of GLUT2 was done using cellSens Imaging Software. The experiment was repeated three times with similar results. Olympus BX-51 upright fluorescent microscope was used to capture images.

Extracellular flux analysis of mitochondrial and glycolytic metabolism

The Seahorse Bioscience XFe96 Flux analyser was used according to the instructions of the manufacturer. The mitochondrial and glycolytic stress test kits used were optimized as described by Krause et al. (2014) to ensure the lowest concentration and maximum effect. The data collected was analysed as described by Chen et al. (2016) and Keane et al. (2015). Basal respiration was determined by deducting the minimum oxygen consumption rate (OCR) after adding rotenone and antimycin A (non-mitochondrial respiration), from the OCR measurement taken immediately before oligomycin addition. Calculation of proton leak was done by deducting non-mitochondrial respiration from the OCR measurement after oligomycin injection. ATP production linked to OCR was determined by the difference between proton leak and basal respiration. Maximum respiration was calculated by deducing the OCR of non-mitochondrial respiration from the maximum OCR after carbonyl cyanide p-crifluoromethoxyphenylhydrazone (FCCP) addition. Reserve capacity was determined from the difference between the basal respiration and maximum respiration. Glycolysis was calculated as the difference between the maximum extracellular acidification rates (ECAR), after the inclusion of glucose, and the ECAR before the addition of glucose. Glycolytic capacity was calculated by subtracting the minimum ECAR, after 2DG addition, from the maximum ECAR, after oligomycin injection. The glycolytic reserve was calculated as the difference between the glycolytic capacity and glycolysis.

Intracellular ATP measurement

BRIN-BD11 cells were grown in 96-well plates for 24h. The concentration of ATP released was measured using a CellTiter-Glo® luminescent assay (Promega Corporation, Madison, WI, USA), following the manufacturer's protocol.

Measurement of calcium influx

Calcium was measured with a Fluo-4 AM calcium indicator using confocal microscopy. The present study used a modified method of Maffucci et al. (2009). In brief, BRIN-BD11 cells (50,000 cells/ well) were plated in a 6-well plate. The growth medium was removed after 24h and replaced with serum-free medium for 6h. After 6h, the cells were incubated for 45min with 4 mM Fluo-4-AM dye (Life Technologies Australia Pty Ltd.) in 2mL of Gibco Hank's balanced salt solution (HBSS) (Thermo Fisher Scientific) at 37°C. Cells were then incubated for 30min in HBSS containing 1.1mM glucose. After a wash, the cells were stimulated with 5.5mM glucose with or without the *T. polium* extract (500µg/mL) or gliclazide (5µM) in KRB buffer. Images were acquired using an Ultraview Vox spinning disk confocal microscope (at 20X objective) equipped with a chamber for live imaging, using the Volocity software (Perkin Elmer, USA). The intensity of Fluo-4 AM calcium fluorescence was measured using ImageJ ® software (Ver. 1.50i).

Statistical analyses

Each experiment was performed multiple times (indicated in each legend) with, at least, 3 replicates each time. Differences in the response between the different treatments were examined using one-way ANOVA or t-tests as appropriate. A General Linear Model (GLM) was used to explore the relationship between the dose of *T. polium* extract and insulin release. In this model, the insulin release (dependent variable) was modelled as a function of the dose (either as µg/mL, or its logarithm). The analysis was performed using GraphPad prism software (6.0, GraphPad prism Software Inc, CA, USA). A p-value < 0.05 was taken to indicate a statistically significant association in all tests.

RESULTS

Extract effect on cell viability

The cytotoxicity of the total extract of *T. polium* was assessed by measuring BRIN-BD11 cell viability following 24h exposure using the MTT and APH assays (Figure 1). Concentrations up to 1mg/mL of the *T. polium* extract did not significantly affect cell viability.

  BRIN-BD11 cells were cultured as described in the methods section. The cells were treated for 24h with 0 to 1mg/mL of the *T. polium* extract. The viability of cells following the treatment was assessed using the (A) MTT and (B) acid phosphatase (APH) assays. All values are
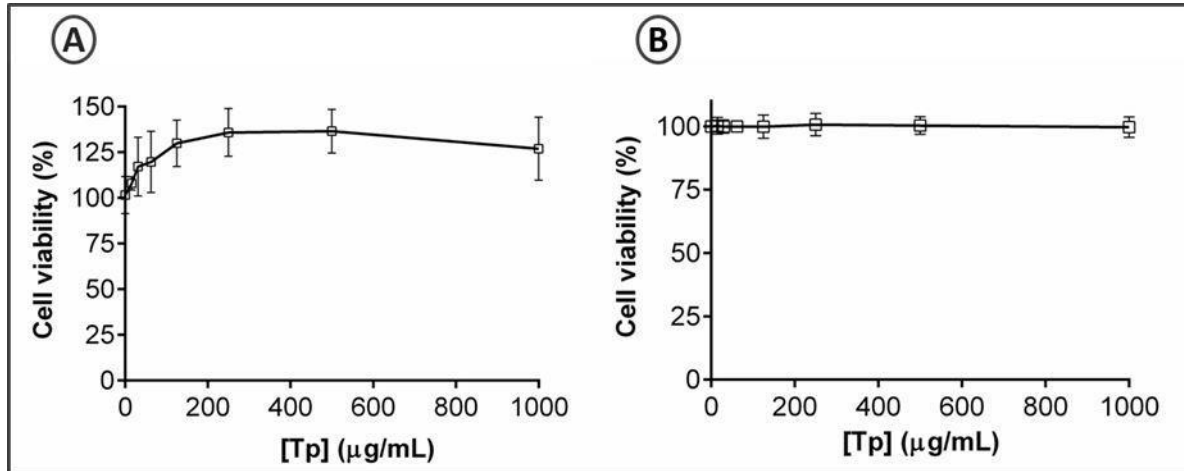
Figure 1. Viability of BRIN-BD11 cells in response to various doses of the *T. polium* extract. BRIN-BD11 cells were cultured as described in the methods section. The cells were treated for 24h with 0 to 1mg/mL of the *T. polium* extract. The viability of cells following the treatment was assessed using the (A) MTT and (B) acid phosphatase (APH) assays. All values are reported as the mean (± SD) of three separate experiments, with each point done in triplicate for each experiment.

reported as the mean (± SD) of three separate experiments, with each point done in triplicate for each experiment.

Extract promoting insulin secretion

Insulin secretion by the total extract of *T. polium* was compared to the effect of gliclazide. The total extract significantly ($p < 0.05$) promoted insulin secretion, and the GLM analysis identified a strong positive association between the dose of the extract and the insulin response ($F_{1,46} = 38.5$; $R^2 = 0.46$; $\beta = 0.0022$; $p < 0.0001$). When the independent variable was changed to Log (dose), the fit of the model was similar ($R^2 = 0.47$). This indicates a concentration-dependent effect from BRIN-BD11 cells, giving a similar insulin release profile to that demonstrated by gliclazide (Figure 2).

Extract enhances glucose uptake

The effect of the *T. polium* extract on glucose uptake by BRIN-BD11 cells was investigated in an independent assay, monitoring the uptake of a fluorescent D-glucose analogue, 2NBDG. The *T. polium* extract (500µg/mL) significantly ($p < 0.001$) promoted 2NBDG uptake into BRIN-BD11 cells within 30min of treatment (Figure 3).

Extract stimulates GLUT2 and glucokinase expression

Western Blot measurement of glucokinase revealed a significant ($p < 0.05$) increase (1.9-fold) in its expression in
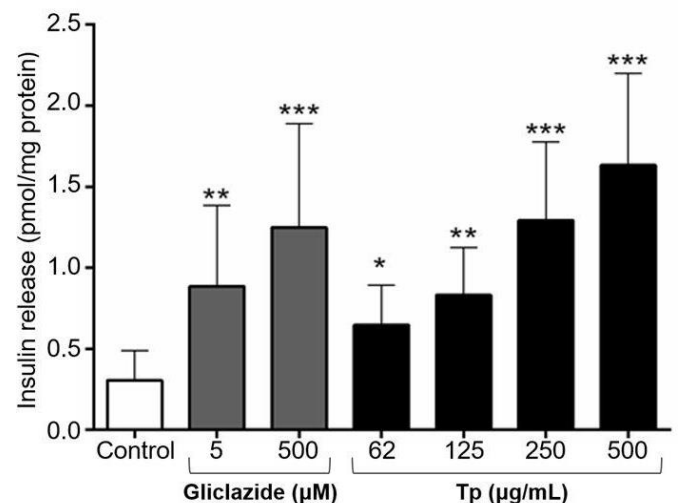
Figure 2. Insulin secretion from BRIN-BD11 cells in response to various concentrations of either *T. polium* extract or gliclazide. The data was normalized to the amount of protein in the cells using a BCA protein quantification assay. All values are reported as the mean (± SD) of four separate experiments, with each point carried out in triplicate for each experiment. Statistical differences (* denotes $p < 0.05$, ** $p < 0.01$, *** $p < 0.001$) between the treatments compared to control (glucose alone) are depicted above. There appears to be a dose-dependent increase ($p < 0.001$) in insulin secretion with extract.

BRIN-BD11 cells in response to the T. polium extract treatment compared to control (Figure 4A and 4B). Additionally, GLUT2 protein levels were also significantly ($p < 0.05$) enhanced by 1.5-fold following treatment with the extract (Figure 4A and 4C). GLUT2 expression of BRIN-BD11 cells was also visualized by
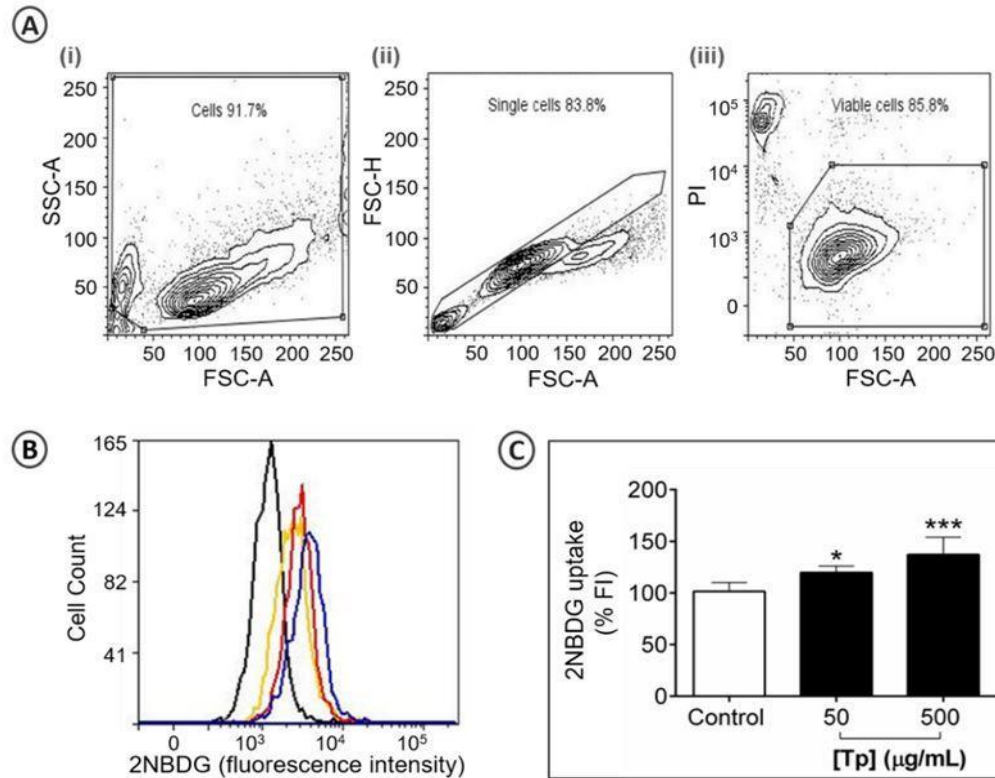
Figure 3. Flow cytometric determination of glucose (2NBDG) uptake by BRIN-BD11 cells following treatment with *T. polium* extract. The Figures in **(A)** depict the flow cytometry gating strategy. Cellular events were gated through (i) the forward scatter (FSC- A) versus the side scatter (SSC-A) plot, and further interrogated by (ii) the ratio of area to height in forward scatter (FSC) to allow for the analysis of single cellular events followed by (iii) the exclusion of propidium iodide to gate out dead cells. The remaining live cells were assessed for glucose uptake measurement. The figures in **(B)** and **(C)** are the results of the serum-starved BRIN-BD11 cells treated for 30min with DMEM media ▮ or the *T. polium* extract (*T. polium*: 50 ▮, 500 ▮ µg/mL) each supplemented with 2NBDG, or a blank ▮ (cells with media but without 2NBDG). Following treatment, the cells were washed, detached with trypsin and stained with propidium iodide. 2NBDG uptake was measured using a flow cytometer. The peak shift of fluorescence intensity (FI) after various treatments are shown in caption **(B)** (▮ control, ▮50µg/mL *T. polium* and ▮500µg/mL *T. polium*) which are quantitated in caption **(C)**. The values in **(C)** are given as percent FI, relative to control. All values are reported as the mean (± SD) of four separate experiments (each point done in triplicate for each experiment). Statistical differences between the treatments were assessed as described in the methods section; * denotes $p<0.05$ and *** $p<0.001$ compared to the control.

immunofluorescence staining after the T. polium extract treatment (Figure 5A). GLUT2 staining increased significantly ($p<0.01$) by 2.4-fold in the presence of the T. polium extract compared to the control treatment (Figure 5B). The merged Figures (Figure 5A, captions v and vi) indicate that this staining coincides with DAPI staining (Figure 5A, captions iii and iv) and confirms that the presence of the GLUT2 was cell-specific.

Stimulatory role of extract on glycolysis

To determine the effects of the *T. polium* extract on beta cell glycolysis, we measured the ECAR of BRIN-BD11 cells after a 30min pre-treatment with the total extract

(Figure 6). Using this approach, we demonstrated a substantially enhanced response of BRIN-BD11 cells to both glucose and oligomycin by increasing the extracellular acidification rate compared to control untreated cells. Calculation of glycolytic rate, glycolytic capacity and non-glycolytic acidification from ECAR measurements indicated a significant ($p<0.05$) increase in all parameters by the *T. polium* extract treatment.

Extract enhances mitochondrial respiration and ATP production

A mitochondrial stress test was employed to measure the oxygen consumption rate following the addition of various
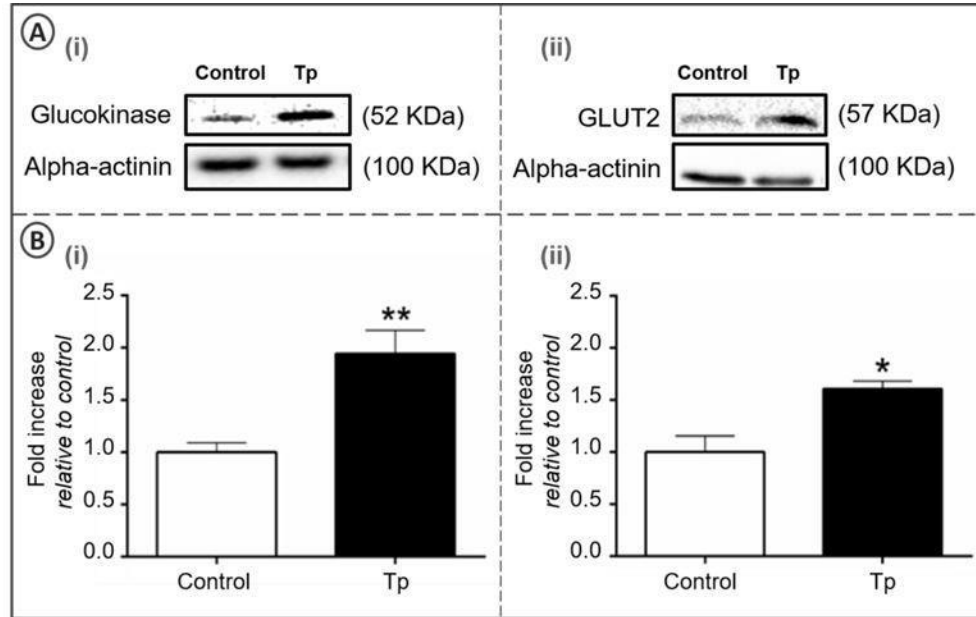
Figure 4. Effect of the *T. polium* extract on glucokinase and glucose transporter 2 (GLUT2) expression in BRIN-BD11 cells. BRIN-BD11 cells were cultured then glucose starved for 40min in KRB buffer containing 1.1 mM glucose. Cells were then treated for 30min with control glucose (5.5mM), or, *T. polium* extract (500µg/mL in 5.5mM glucose). Cell lysates were collected and used for Western Blot. **(A)** Glucokinase (i) and GLUT2 (ii) were present in BRIN-BD11 after treatment with *T. polium* extract and control media. **(B)** Level of glucokinase upregulation (i) and GLUT2 upregulation (ii) by *T. polium* extract. α-Actinin was used as a housekeeping control. All data are presented after normalising with α-actinin expression and are expressed relative to the control. All values are reported as the mean (± SD) of four separate experiments, with each point done in triplicate for each experiment. Statistical differences between the treatments were assessed as described in the methods section; * denotes $p < 0.05$ and ** $p < 0.01$ compared to control.

modulators of mitochondrial function (Brand and Nicholls, 2011). This strategy allowed the determination of various mitochondrial parameters including basal respiration, maximal respiration and spare respiratory capacity. The oxygen consumption rate (OCR) measurements indicated that all the mitochondrial bioenergetics parameters were significantly ($p<0.05$) increased in the presence of the *T. polium* extract for 30min (Figure 7A and 7B).

In addition, intracellular ATP levels in BRIN-BD11 cells were measured after exposure to the *T. polium* extract (500µg/mL) or alanine (10mM) for 30min (Figure 8A). The *T. polium* extract and Alanine, another known insulin secretagogue significantly ($p<0.01$) promoted intracellular ATP generation from BRIN-BD11 cells compared to the control. As was observed in Figure 8A, the amount of ATP produced in the mitochondria, independently calculated from extracellular flux analysis (last rate measurement before oligomycin injection minus minimum rate measurement after oligomycin injection), was also significantly ($p < 0.05$) enhanced (Figure 8B).

Extract promoting intracellular calcium influx

Calcium influx in BRIN-BD11 cells was monitored using confocal microscopy (Figure 9). To assess interference between the extract and the dye, the cells were incubated with (1) the *T. polium* extract in the absence of the Fluo-4 AM dye and, separately (2) the Fluo-4 AM dye alone. There was a sharp increase in the calcium influx after treatment with *T. polium* extract or gliclazide, compared with control (Figure 9B). Using immunofluorescence microscopy, a significant ($p < 0.01$) increase in the intracellular calcium was observed after treatment with 5µM gliclazide or the *T. polium* extract (500µg/mL) in the presence of 5.5mM glucose solution, respectively (Figure 9A).

Quantitation of key constituents

The amount of apigenin, quercetin and rutin were quantitated to compare activity levels achieved by using the extract to the concentrations used by other authors who examined each of these pure compounds in cell culture models (Cazarolli et al., 2009a; Cazarolli et al., 2009b; Erraught et al., 2016; Kittl et al., 2016; Ghorbani, 2017). Dried extract from 1g of plant material was reconstituted in hot water and analysed by LCMS (Figure 10) as outlined in the methods section. Although this
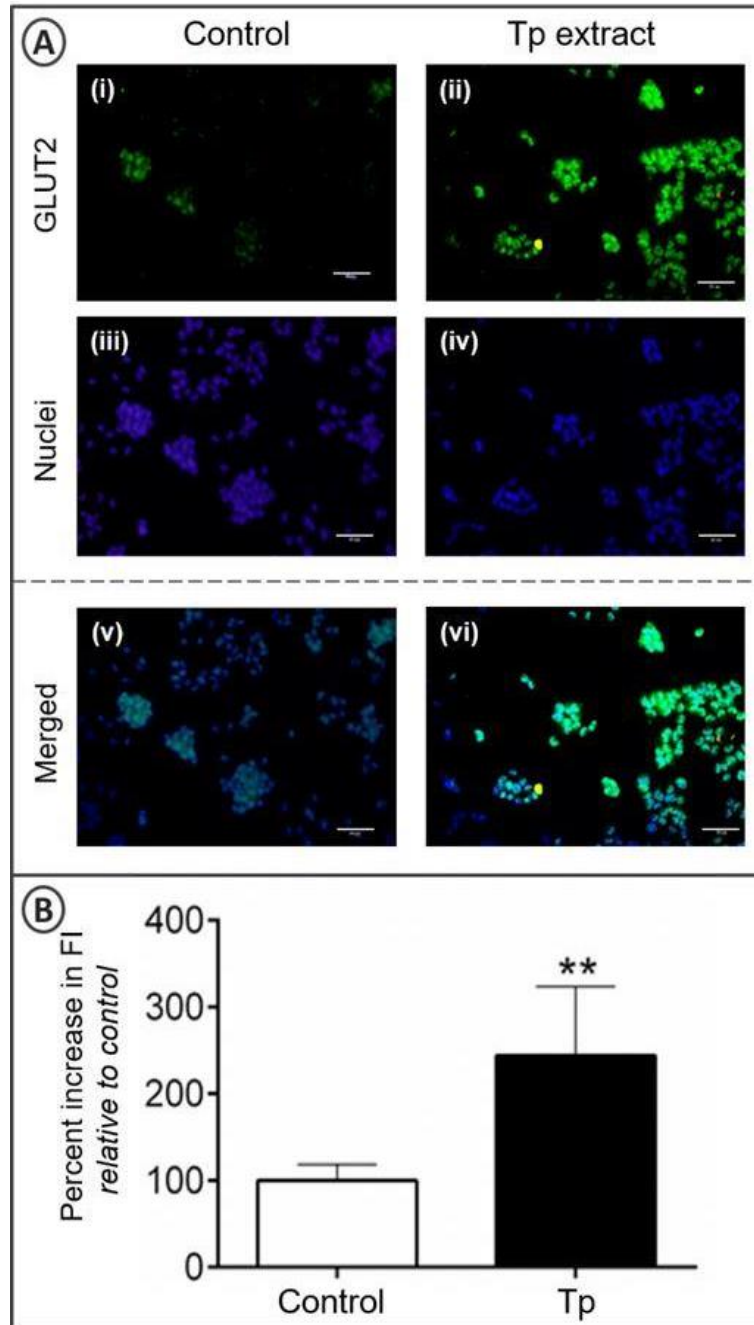
Figure 5. Confocal microscopy imaging of GLUT2 in BRIND-BD11 cells treated with the *T. polium* extract. BRIN-BD11 cells were cultured as described in the methods section. Cells were glucose starved for 40min in KRB buffer containing 1.1mM glucose. Cells were then treated for 30min with 5.5mM glucose (control) or *T. polium* extract (500µg/mL in 5.5mM glucose) in KRB buffer. **(A)** Cells were stained with antibodies and observed in an Olympus upright microscope to obtain images of GLUT2 (i), (ii) and DAPI nuclear staining (iii), (iv). Merged pictures of both GLUT2 and nuclei in control and the *T. polium* extract (500µg/mL) treated cells are shown in caption (v) and (vi), respectively. The scale bar corresponds to 50µm. **(B)** Fluorescence intensity of GLUT2 observed (green fluorescence) in BRIN-BD11 cells shown in caption **(A)** was measured using ImageJ ® software (Ver. 1.50i). The experiment was repeated three times with similar results. A representative result of one experiment is shown here. ** denotes p<0.01 compared to control.
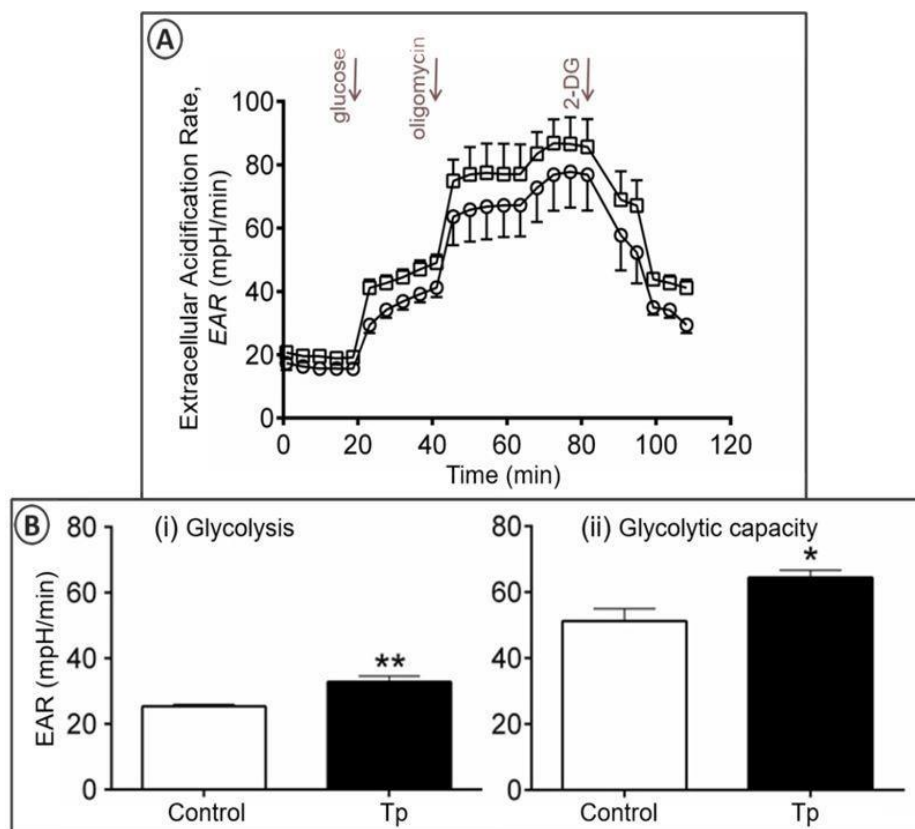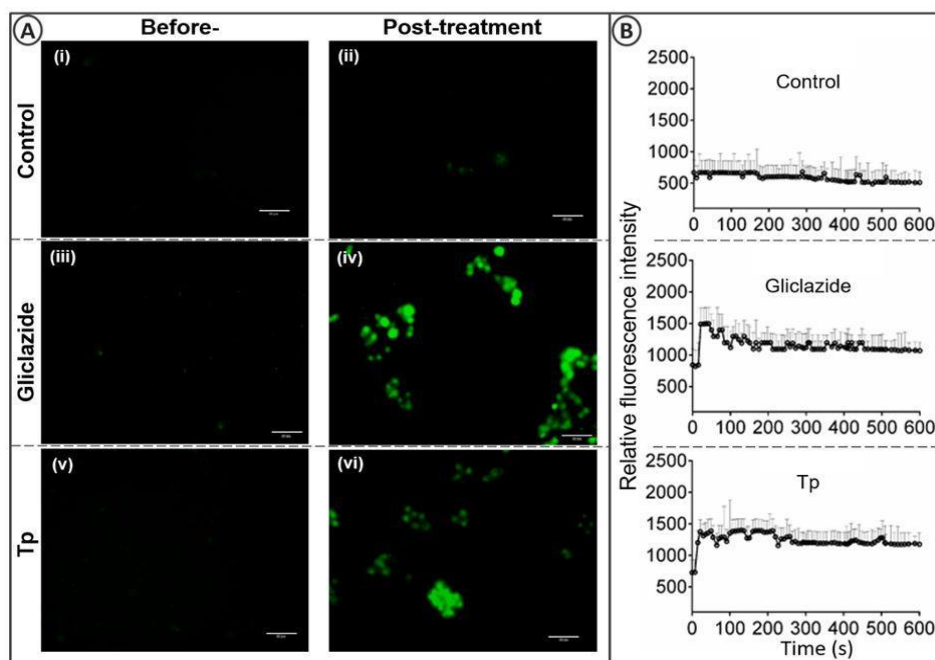
Figure 6. The effect of the *T. polium* extract on a glycolysis stress test in BRIN-BD11 cells. BRIN-BD11 cells were seeded and cultured for 24h as described in the methods section. On the day of the experiment, BRIN-BD11 cells were pre-treated for 30min with control KRB buffer or T. polium extract (500µg/mL). **(A)** The extracellular acidification rate (ECAR) was measured under basal conditions and sequentially over 120min with the addition of 25mM glucose, oligomycin and 2 Deoxyglucose (2DG) at set time points. ECAR was monitored over 120min. Individual parameters for the glycolytic stress test are shown in **(B)**: (i) Glycolysis and ii) Glycolytic capacity which were calculated as outlined in the methods section. All values are reported as the mean (± SD) of four separate experiments, with each point done in triplicate for each experiment; * denotes p<0.05 and **p<0.01 compared to control.
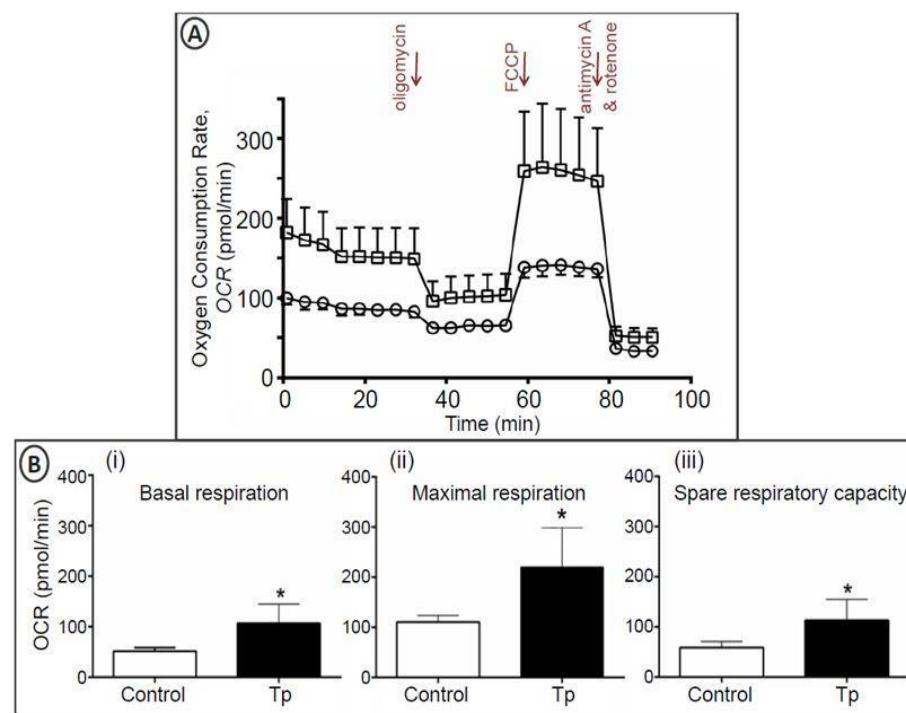
Figure 7. Effect of the *T. polium* extract on bioenergetics and mitochondrial metabolism in BRIN-BD11 cells. **(A)** Oxygen consumption rate (OCR) of mitochondria after *T. polium* extract or vehicle control treatment was monitored. **(B)** Individual parameters for (i) basal respiration, (ii) maximal respiration, and iii) spare respiratory capacity were calculated as outlined in the methods section. All values are reported as the mean (± SD) of four separate experiments, with each point done in triplicate for each experiment. Statistical differences between the treatments were assessed; * denotes p<0.05 compared to control.
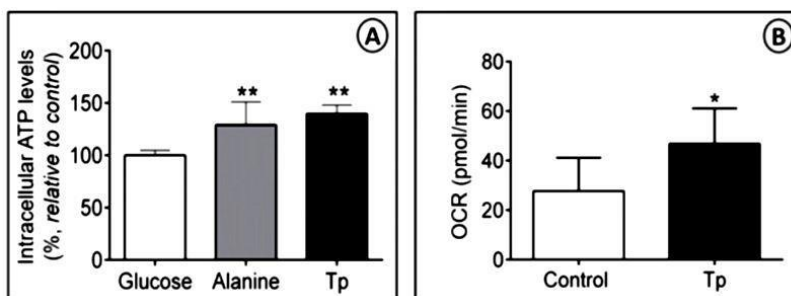
Figure 8. Intracellular ATP levels of BRIN-BD11 cells in Cell-Titer Glo luminescent assay and Sea horse mitochondrial XF stress test. **(A)** Using the Cell-Titer Glo Luminescent assay, ATP concentrations were measured. The ATP levels are presented as a percentage of control; control levels are set at 100%. The cells were treated with 5.5mM glucose (control), 10mM alanine in KRB buffer containing 16.7mM glucose (positive control) or *T. polium* extract (500µg/mL) in KRB buffer containing 5.5mM glucose for 30min. **(B)** In the seahorse mitochondrial stress test, the oxygen consumption rate (OCR) of mitochondria after treatment with the *T. polium* extract or vehicle control was monitored and the ATP released was calculated as outlined in the methods section. All values are reported as the mean (± SD) of four separate experiments, with each point done in triplicate for each experiment; Statistical differences between the treatments compared to the control (5.5mM glucose) were assessed; ** denotes p<0.01.

Figure 9. The effect of *T. polium* extract on calcium influx in BRIN-BD11 cells imaged by confocal microscopy. BRIN-BD11 cells were stained with Fluo-4 AM dye and treated as outlined in the methods section. **(A)** Images were taken before (i, iii, v) and 30 seconds after (ii, iv, vi) the addition of 5.0µM gliclazide (iv) or 500 µg/mL *T. polium* extract (vi) using Perkin-Elmer confocal microscope. Green fluorescence indicates the presence of calcium inside the cells. The scale bar corresponds to 50µm. The experiment was repeated three times with similar results. A representative image of one experiment is shown here. **(B)** The time course of intracellular calcium binding with internalized Fluo4-AM dye was monitored using a Perkin-Elmer confocal microscope. Fluorescence of calcium at various time points (0-600 seconds) was observed and measured as outlined in the methods section. All values are reported as the mean (± SD) of three separate experiments, with each point done in triplicate for each experiment.
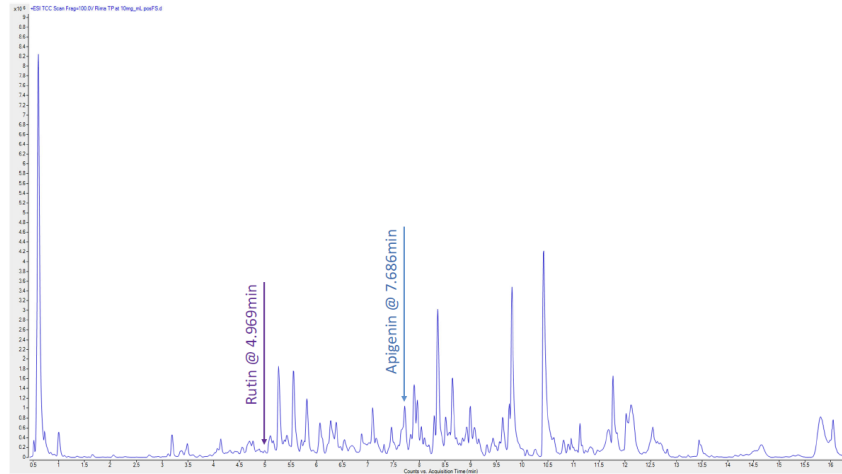
Figure 10. The total ion chromatogram (TIC) scan of the *T. polium* extract in +ESI mode. Apigenin and rutin were confirmed with reasonable certainty by matching extracted ion chromatogram signals of the extract with accurate mass, retention time and MSMS fragmentation of pure compounds.

method enabled us to measure the amount of apigenin (10.92μg) and rutin (10.32μg) from 1 gram of *T. polium*, quercetin was not detected.

DISCUSSION

Our current study confirms initial findings suggesting that extracts of *T. polium* lower blood glucose by increasing insulin release from pancreatic beta cells (Figures 2 and 3). This was further confirmed by significant increases in glucokinase and GLUT2 expression (Figures 4 and 5). These findings were further confirmed by significant increases, in *T. polium* treated cells, in key metabolic markers (Figures 6-9) of pancreatic beta cell activity necessary for insulin secretion. The extract has been found to contain compounds of insulinotrophic potential (Figure 10) (Ireng et al., 2016) as have been individually investigated as pure compounds by others and independently shown to promote insulin secretion (Kittl et al., 2016; Ghorbani, 2017; Cazarolli et al., 2009a).

In the current study, the *T. polium* extract promoted insulin secretion from BRIN-BD11 pancreatic beta cells in a dose-dependent manner (Figure 2) which is in line with previous reports (Kasabri et al., 2012; Mirghazanfari et al., 2010; Stefkov et al., 2011). Stefkov et al. (2011) reported that an ethanol extract of *T. polium* promoted a 2.6-fold, dose-dependent increase in insulin release by MIN6 pancreatic beta cells in the presence of 20mM glucose. Kasabri et al. (2012) reported that an aqueous extract of *T. polium* promoted a 19-fold increase in insulin release by MIN6 in the presence of 5.6mM glucose. Mirghazanfari et al. (2010) reported that a methanolic extract of *T. polium* potentiated glucose-stimulated release of insulin, from basal level, significantly

($p<0.0001$), giving a 23 and 44-fold increase in insulin release from *in situ* rat pancreas perfused in 2.8 and 16.7mM glucose, respectively. Collectively, these previous studies and the present study provide compelling evidence that constituent(s) within the *T. polium* extract promote insulin secretion.

The *T. polium* extract significantly ($p<0.05$) increased glucose uptake into BRIN-BD11 cells as measured by two independent assays: the glucose uptake assay (Figure 3) and the glucose consumption assay (results not shown). This significant glucose uptake was detected within 30min of treatment which also coincided with increased expression of GLUT2 following treatment of these cells with the *T. polium* extract (Figures 4 and 5). In addition to promoting GLUT2 expression, the *T. polium* extract significantly ($p < 0.01$) increased the expression of glucokinase (Figure 4). These findings are in agreement with the key role GLUT2 plays in the fast uptake of glucose into beta cells (Fu et al., 2013; Tal et al., 1992) followed by its rapid phosphorylation by glucokinase (Matschinsky et al., 1993) Further, our results are in support with previous report on *T. polium* extract promoting the activity of glucokinase in the liver of diabetic rats (Stefkov et al., 2011; Vessal et al., 2003), and consistent with the effect of *T. polium* in promoting insulin secretion (Bahramikia and Yazdanparast, 2012) .

The increased expression of both GLUT2 and glucokinase is consistent with the effect of *T. polium* in promoting insulin secretion. Increased transport of glucose into cells via GLUT2 and commitment of glucose to glycolysis by the action of glucokinase can potentiate insulin secretion through an increased ATP/ADP ratio as well as by generation of other coupling factors during oxidative phosphorylation. This conclusion assumes that the GLUT2/glucokinase sensor system in BRIN-BD11

cells is the rate-limiting step in this process, an assumption which is supported by several studies (Mirghazanfari et al., 2010; Schuit et al., 2001; Tal et al., 1992).

It might be informative to explore whether the *T. polium* extract promotes increased expression of GLUT2 at the plasma membrane. It should be noted that whilst the current study shows GLUT2 expression is increased, this does not necessarily guarantee that the increased expression translates to increased translocation at the plasma membrane where it is needed to facilitate glucose transport into the beta cell. Although Figure 5 illustrates fluorescently tagged GLUT2 in beta cells, these experiments did not enable actual cellular localisation of the transporter molecules. Future studies might focus on microscopy experiments on transfected beta cells using subcellular compartment reporters (Ait-Omar et al., 2011; Cohen et al., 2014), endosome markers or studies on loss of function of GLUT2 (e.g. siRNA knockdown) (Low et al., 2021; Ohtsubo et al., 2011) to enable localisation of the transporters to be determined.

In keeping with the observation that the *T. polium* extract promotes glucose transport through increased expression of GLUT2 and glucokinase, it might be expected that this leads to the increased phosphorylation of glucose, which thereby commits glucose to glycolytic processing within these beta cells (Mithieux et al., 2004). The speculation that the *T. polium* extract does indeed promote glycolytic processing of glucose is supported by a Seahorse XF glycolysis stress test (Figure 6). The constituents of the *T. polium* extract increased the extracellular acidification rate (Figure 6A) and glycolytic rate (Figure 6B) via glucose uptake (Figure 3), which is important for energy metabolism (Figure 7). Further studies on mRNA and protein expression of other key glycolytic genes are necessary to explore the detailed mechanism of the constituents of the *T. polium* extract on the glycolytic pathway.

It would be expected that if the glycolytic capacity of beta cells is enhanced by the *T. polium* extract, there is either increased production of lactate, as an end-point of glycolysis or that pyruvate enters the mitochondrial pathways (tricarboxylic acid cycle and oxidative phosphorylation). Lactate measurements were not performed in the current study; however, beta cells typically express very low levels of lactate dehydrogenase(Ainscow et al., 2000; Sekine et al., 1994). The mitochondrial stress test data support the conclusion that the *T. polium* extract enhances mitochondrial respiration (Figures 7A and 7B). The extract promoted basal respiration in mitochondria, which indicates that AT. POLIUM turnover in the cells and non-mitochondrial respiration were increased (Figure 7). The pyruvate and NADH from glycolytic and mitochondrial metabolism are important for glucose-stimulated insulin secretion and its regulation (Campbell and Newgard, 2021; Rutter et al., 2015). There was a significant ($p <$

0.05) increase in maximal mitochondrial respiration after the *T. polium* extract treatment (Figure 7B), which in turn enhances substrate availability for the respiratory chain (Brand and Nicholls, 2011; Ruas et al., 2016). Previously, Baali et al. (2016) reported an increase in mitochondrial respiration in rat liver after chronic treatment with *T. polium* extract *in vivo*. Although this group measured the hepatic mitochondrial bioenergetics using high-resolution Oxygraph-2K, their data is in line with the findings of the current study reporting an upregulation of mitochondrial respiration in pancreatic beta cells following treatment with the *T. polium* extract.

Upregulation of glycolytic activity and mitochondrial respiration should lead to an increase in oxidative phosphorylation and ATP production in the cells (Campbell and Newgard, 2021; Sekine et al., 1994). Indeed, as would be expected, the treatment of BRIN-BD11 cells with the *T. polium* extract promoted ATP production in BRIN-BD11 cells (Figure 8). This finding was verified in two independent assays: mitochondrial stress test and Celltiter-Glo luminescent assay. The increased production of ATP in the presence of the *T. polium* extract would increase the ATP: ADP ratio to facilitate the closure of the K_{ATP} (Campbell and Newgard, 2021; Miguel et al., 2004; Ruas et al., 2016). This should lead to membrane depolarization and the opening of calcium channels (Haythorne et al., 2019; Tarasov et al., 2004). In the current study, although the effect of the *T. polium* extract on K_{ATP} channel closure was not investigated, calcium influx into the beta cells, which is a consequence of K_{ATP} channel closure, was observed. As would be expected with increased intracellular ATP production, the *T. polium* extract increased intracellular calcium influx in BRIN-BD11 (Figure 9). Our results here are in agreement with a previous study which found that diazoxide, a K_{ATP} channel opening agent, and verapamil, a calcium channel blocker, inhibit the *T. polium* extract promoted insulin secretion in perfused rat pancreas (Mirghazanfari et al., 2010). The authors of this study concluded that constituents of the *T. polium* extract act on K_{ATP} channels and calcium channels; however, may not be acting directly on these channels.

The precise compound(s) responsible for the glucose-lowering effect of the total extract of *T. polium* are yet to be identified. Meanwhile, there have been several studies that examined the total plant extract for its glucose-lowering effect (Bahramikia and Yazdanparast, 2012; Mirghazanfari et al., 2010; Vessal et al., 2003) and some studies attempted to examine the activity of certain pure compounds, namely apigenin, quercetin and rutin (Cazarolli et al., 2009b; Haythorne et al., 2019; Kittl et al., 2016) that have been putatively identified in *T. polium* (Ireng et al., 2016). However, it is important to remember that studies testing isolated flavonoids in cell culture optimise the concentrations used depending on cell viability assays, therefore most likely lead to the amounts tested far exceeding actual individual compound

concentrations in the extract (Kittl et al., 2016; Stefkov et al., 2011). In our current extract we were unable to detect quercetin (Figure 10) and the concentrations of apigenin and rutin (~5ng/mL on cells in culture) in the extract appear to be much lower than what is necessary (500ug/mL) to deliver significant differences in responses in activity experiments using single flavonoids in culture (Kappel et al., 2013). However, these initial quantities may be underestimates since our method used external standards which do not account for sink conditions brought about by the total extract medium. Nonetheless, the extract from 62µg of *T. polium* aerial parts significantly (p<0.05) increased insulin secretion *in vitro* (Figure 2). In light of these findings, more work is necessary to examine the constituents of the *T. polium* extract further. Future studies should also investigate whether quercetin is solely present in the form of rutin and examine *T. polium* for glucose-lowering compounds. Additionally, the aglycones and human metabolites may be of more relevance to *in vivo* scenarios since the glycosides are usually hydrolysed upon ingestion, and rapidly metabolised *in vivo* generating several methylated, sulfonated and glucuronidated forms, which may contribute to *in vivo* activity (Kappel et al., 2013; Manach et al., 1998).

As demonstrated in the present study, treatment of BRIN-BD11 cells with the *T. polium* extract promotes GLUT2 (Figures 4 and 5) and glucokinase (Figure 4) expression, which appear to have led to the increased glycolytic activity (Figure 6) and mitochondrial respiration (Fig 7), consequently resulting in increased ATP production (Figure 8), presumably inhibiting potassium efflux and thereby promoting calcium influx (Figure 9). Studies evaluating the effects of *T. polium* extract on isolated ion channels (including various voltage-gated calcium channels) (Braun et al., 2008; Soares et al., 2017; Rorsman and Ashcroft, 2018) may be needed in future to determine whether constituent(s) of the *T. polium* extract interact directly with various ion channels. This study thus suggests that the *T. polium* extract contains compounds that promote insulin secretion in BRIN-BD11 cells by inducing the glucose sensing/metabolising pathways.

CONCLUSION

Our current findings indicate that constituents(s) within the *T. polium* extract promote insulin secretion by promoting GLUT2 and glucokinase expression. The increased expression of both glucokinase and GLUT2 in beta cells is particularly noteworthy as these activities constitute the glucose sensor of pancreatic beta cells and have a high impact on glucose homeostasis, which is impaired in type 2 diabetes. Furthermore, this led to increased glucose transport, metabolism, ATP production and ultimately Ca^{2+} influx following the well-established biochemical pathway for insulin release from pancreatic

beta cells. Flavonoids within the extract are of growing interest; however, it is important to determine the total amounts of each constituent considering the different glycosides, human metabolites and their concentrations *in vivo*, when assessing flavonoid activities *in vitro*, especially since the activities of ingested compounds may vary upon metabolism. Therefore, the *T. polium* extract appears an impactful target for future drug discovery efforts for the treatment of type 2 diabetes and related disorders; however, the approach in assessing the constituents may very much influence their selection.

REFERENCES

Abdollahi M, Karimpour H, Monsef-Esfehani HR, **2003**. Antinociceptive effects of *Teucrium polium L.* total extract and essential oil in mouse writhing test. Pharmacol Res, 48: 31-35.

Ainscow EK, Zhao C, Rutter GA, **2000**. Acute overexpression of lactate dehydrogenase-A perturbs beta-cell mitochondrial metabolism and insulin secretion. Diabetes, 49: 1149-1155.

Ait-Omar A, Monteiro-Sepulveda M, Poitou C, Le Gall M, Cotillard A, Gilet J, Garbin K, Houllier A, Château D, Lacombe A, Veyrie N, Hugol D, Tordjman J, Magnan C, Serradas P, Clément K, Leturque A, Brot-Laroche E, **2011**. GLUT2 accumulation in enterocyte apical and intracellular membranes. Diabetes, 60(10): 2598-2607. doi: 10.2337/db10-1740.

Albadr Y, Crowe A, Caccetta R, **2022**. *Teucrium polium*: Potential Drug

Source for Type 2 Diabetes Mellitus. MDPI Biology, 11(1): 128. doi: 10.3390/biology11010128. PMID: 35053127; PMCID: PMC8772689.

Ardestani A, Yazdanparast R, Jamshidi S, 2008. Therapeutic effects of *Teucrium polium* extract on oxidative stress in pancreas of streptozotocin-induced diabetic rats. J Med Food, 11: 525-532.

Ashcroft FM, Harrison DE, Ashcroft SJ, 1984. Glucose induces closure of single potassium channels in isolated rat pancreatic β-cells. Nature, 312: 446-8.

Baali N, Belloum Z, Baali S, Chabi B, Pessemesse L, Fouret G, Ameddah S, Benayache F, Benayache S, Feillet-Coudray C, Cabello G, Wrutniak-Cabello C, 2016. Protective activity of total polyphenols from *Genista quadriflora* Munby and *Teucrium polium geyrii* Maire in acetaminophen-induced hepatotoxicity in rats. Nutrients, 8(4): 193. PubMed PMID: 27043622; PubMed Central PMCID: PMC4848662.

Bahramikia S, Yazdanparast R, 2012. Phytochemistry and medicinal properties of *Teucrium polium L.* (Lamiaceae). Phytother Res, 26: 1581-1593.

Brand MD, Nicholls DG, 2011. Assessing mitochondrial dysfunction in cells. Biochem J, 435: 297-312.

Braun M, Ramracheya R, Bengtsson M, Zhang Q, Karanauskaite J, Partridge C, Johnson PR, Rorsman P, 2008. Voltage-gated ion channels in human pancreatic β-cells: electrophysiological characterization and role in insulin secretion. Diabetes, 57: 1618-1628.

Campbell JE, Newgard CB, 2021. Mechanisms controlling pancreatic islet cell function in insulin secretion. Nat Rev Mol Cell Biol, 22: 142–158. https://doi.org/10.1038/s41580-020-00317-7.

Capasso F, Cerri R, Morrica P, Senatore F, 1983. Chemical composition and anti-inflammatory activity of an alcoholic extract of *Teucrium polium* L. Boll Soc Ital Biol Sper, 59: 1639-1643.

Carlessi R, Chen Y, Rowlands J, Cruzat VF, Keane KN, Egan L, Mamotte C, Stokes R, Gunton JE, Bittencourt PIH, Newsholme P, 2017. GLP-1 receptor signalling promotes beta-cell glucose metabolism via mTOR-dependent HIF-1alpha activation. Sci Rep, 7: 2661. PubMed PMID: 28572610; PubMed Central PMCID: PMC5454020.

Cazarolli LH, Folador P, Moresco HH, Brighente IMC, Pizzolatti MG, Silva FR, 2009b. Stimulatory effect of apigenin-6-C-β-l-fucopyranoside on insulin secretion and glycogen synthesis. Eur J Med Chem, 44: 4668-4673.

Cazarolli LH, Folador P, Moresco HH, Brighente IMC, Pizzolatti MG, Silva FR, 2009a. Mechanism of action of the stimulatory effect of apigenin-6-C-(2''-O-alpha-l-rhamnopyranosyl)-beta-L-fucopyranoside on 14C-glucose uptake. Chem Biol Interact, 179: 407-412.

Chaturvedi V, Dye E, Kinnear BF, van Kuppevelt, TH, Grounds MD, Coombe DR, 2015. Interactions between skeletal muscle myoblasts and their extracellular matrix revealed by a serum free culture system. PloS One, 10(6): e0127675. https://doi.org/10.1371/journal.pone.0127675.

Chen Y, Carlessi R, Walz N, Cruzat VF, Keane K, John AN, Jiang FX, Carnagarin R, Dass CR, Newsholme P, 2016. Pigment epithelium-derived factor (PEDF) regulates metabolism and insulin secretion from a clonal rat pancreatic beta cell line BRIN-BD11 and mouse islets. Mol Cell Endocrinol, 426: 50-60.

Cohen M, Kitsberg D, Tsytkin S, Shulman M, Aroeti B, Nahmias Y, 2014. Live imaging of GLUT2 glucose-dependent trafficking and its inhibition in polarized epithelial cysts. Open Biol, 4(7): 140091. PubMed PMID: 25056286; PubMed Central PMCID: PMC4118605.

Cozzani S, Muselli A, Desjobert JM, Bernardini AF, Tomi F, Casanova J, 2005. Chemical composition of essential oil of *Teucrium polium* subsp. *capitatum (L)* from Corsica. Flavour Fragr J, 20: 436-441.

Dagenais GR, Gerstein HC, Zhang X, McQueen M, Lear S, Lopez-Jaramillo P, Mohan V, Mony P, Gupta R, Kutty VR, Kumar R, Rahman O, Yusoff K, Zatonska K, Oguz A, Rosengren A, Kelishadi R, Yusufali A, Diaz R, Avezum A, Lanas F, Kruger A, Peer N, Chifamba J, Iqbal R, Ismail N, Xiulin B, Jiankang L, Wenqing D, Gejie Y, Rangarajan S, Teo K, Yusuf S, 2016. Variations in diabetes prevalence in low-, middle-, and high-income countries: results from the prospective urban and rural epidemiological study. Diabetes Care, 39: 780-787.

Del Prato S, Bonadonna RC, Bonora E, Gulli G, Solini A, Shank M, De Fronzo, RA, 1993. Characterization of cellular defects of insulin action in type 2 (non-insulin-dependent) diabetes mellitus. J Clin Invest, 91: 484-494.

Erraught C, Kirwan L, Brennan L, 2016. The potential of food derived bioactives for blood glucose management. Proc Nutr Soc, 75(OCE2): E54. doi:10.1017/S0029665116000446

Esmaeili MA, Yazdanparast R, 2004. Hypoglycaemic effect of *Teucrium polium*: studies with rat pancreatic islets. J Ethnopharmacol, 95: 27-30.

Ferre T, Riu E, Bosch F, Valera A, 1996. Evidence from transgenic mice that glucokinase is rate limiting for glucose utilization in the liver. FASEB J, 10: 1213-8.

Friedrich J, Eder W, Castaneda J, Doss M, Huber E, Ebner R, Kunz-Schughart LA, 2007. A reliable tool to determine cell viability in complex 3-d culture: the acid phosphatase assay. J Biomol Screen, 12: 925-37.

Fu Z, Gilbert ER, Liu D, 2013. Regulation of insulin synthesis and secretion and pancreatic Beta-cell dysfunction in diabetes. Curr Diabetes Rev, 9: 25-53.

German MS, 1993. Glucose sensing in pancreatic islet beta cells: the key role of glucokinase and the glycolytic intermediates. Proc Natl Acad Sci, 90: 1781-1785.

Ghorbani A, 2017. Mechanisms of antidiabetic effects of flavonoid rutin. Biomed Pharmacother, 96: 305-312.

Haythorne E, Rohm M, van de Bunt M, Brereton MF, Tarasov AI, Blacker TS, Sachse G, Silva Dos Santos M, Terron Exposito R, Davis S, Baba O, Fischer R, Duchen MR, Rorsman P, MacRae JI, Ashcroft FM, 2019. Diabetes causes marked inhibition of mitochondrial metabolism in pancreatic β-cells. Nat Commun, 10: 2474-2491. https://doi.org/10.1038/s41467-019-10189-x

Ireng A, Helmerhorst E, Parsons R; Caccetta R, 2016. Teucrium polium significantly lowers blood glucose levels acutely in normoglycemic male Wistar rats: A comparative to insulin and metformin. Adv Med Plant Res, 4(1): 1-10.

Kappel VD, Federico MJS, Postal BG, Mendes CP, Cazarolli LH, Silva FRMB, 2013. The role of calcium in intracellular pathways of rutin in rat pancreatic islets: potential insulin secretagogue effect. Eur J Pharmacol, 702: 264-268.

Kasabri V, Abu-Dahab R, Afifi FU, Naffa R, Majdalawi L, Shawash H, 2012. In vitro Modulation of pancreatic MIN6 insulin secretion and proliferation and extrapancreatic glucose absorption by *Paronychia argentea*, *Rheum ribes* and *Teucrium polium* Extracts. Jordan J Pharm Sci, 5: 203-217.

Kauffman KJ, Kanthamneni N, Meenach SA, Pierson BC, Bachelder EM, Ainslie KM, 2012. Optimization of rapamycin-loaded acetalated dextran microparticles for immunosuppression. Int J Pharm, 422: 356-363.

Keane KN, Calton EK, Cruzat VF, Soares MJ, Newsholme P, 2015. The impact of cryopreservation on human peripheral blood leucocyte bioenergetics. Clin Sci, 128: 723-733.

Kittl M, Beyreis M, Tumurkhuu M, Fürst J, Helm K, Pitschmann A, Gaisberger M, Glasl S, Ritter M, Jakab M, 2016. Quercetin Stimulates Insulin Secretion and Reduces the Viability of Rat INS-1 Beta-Cells. Cell Physiol Biochem, 39: 278-293.

Krause M, Keane K, Rodrigues-Krause J, Crognale D, Egan B, De Vito G, Murphy C, Newsholme P, 2014. Elevated levels of extracellular heat-shock protein 72 (eHSP72) are positively correlated with insulin resistance in vivo and cause pancreatic β-cell dysfunction and death in vitro. Clin Sci, 126(10): 739-752.

Leahy JL, Bonner-Weir S, Weir GC, 1992. β-Cell dysfunction induced by chronic hyperglycemia: current ideas on mechanism of impaired glucose-induced insulin secretion. Diabetes Care, 15: 442-455.

Low BSJ, Lim CS, Ding SSL, Tan YS, Ng NHJ, Krishnan VG, Ang SF, Neo CWY, Verma CS, Hoon S, Lim SC, Tai ES, Teo AKK, 2021. Decreased GLUT2 and glucose uptake contribute to insulin secretion defects in MODY3/HNF1A hiPSC-derived mutant β cells. Nat Commun, 12(1): 3133. doi: 10.1038/s41467-021-22843-4. PMID: 34035238; PMCID: PMC8149827.

Maechler P, Wollheim CB, 1999. Mitochondrial glutamate acts as a messenger in glucose-induced insulin exocytosis. Nature, 402: 685-689.

Maechler P, Wollheim CB, 2000. Mitochondrial signals in glucose-stimulated insulin secretion in the beta cell. J Physiol, 529: 49-56.

Maffucci T, Raimondi C, Abu-Hayyeh S, Dominguez V, Sala G, Zachary I, Falasca M, **2009**. A phosphoinositide 3-kinase/phospholipase Cgamma1 pathway regulates fibroblast growth factor-induced capillary tube formation. PloS One, 4(12): e8285. PubMed PMID: 20011604; PubMed Central PMCID: PMC2788267.

Manach C, Morand C, Crespy V, Demigné C, Texier O, Régérat F, Rémésy C, **1998**. Quercetin is recovered in human plasma as conjugated derivatives which retain antioxidant properties. FEBS Lett, 426: 331–336.

Markworth E, Schwantecher C, Schwanstecher M, **2000**. ATP4-mediates closure of pancreatic beta-cell ATP-sensitive potassium channels by interaction with 1 of 4 identical sites. Diabetes, 49: 1413-1418.

Matschinsky F, Liang Y, Kesavan P, Wang L, Froguel P, Velho G, Cohen D, Permutt MA, Tanizawa Y, Jetton TL, et al., **1993**. Glucokinase as pancreatic beta cell glucose sensor and diabetes gene. J Clin Invest, 92: 2092-2098.

Matschinsky FM, **1990**. Glucokinase as glucose sensor and metabolic signal generator in pancreatic β-cells and hepatocytes. Diabetes, 39: 647-652.

McClenaghan N, Barnett C, O'Harte F, Flatt P, **1996**. Mechanisms of amino acid-induced insulin secretion from the glucose-responsive BRIN-BD11 pancreatic B-cell line. J. Endocrinol, 151: 349-357.

Menke A, Casagrande S, Cowie CC, **2016**. US Trends for diabetes prevalence among adults—reply. J Am Med Assoc, 315: 705-706.

Miguel JC, Patterson S, Abdel-Wahab YH, Mathias PC, Flatt PR, **2004**. Time-correlation between membrane depolarization and intracellular calcium in insulin secreting BRIN-BD11 cells: studies using FLIPR. Cell Calcium, 36: 43-50.

Mirghazanfari SM, Keshavarz M, Nabavizadeh F, Soltani N, Kamalinejad M, **2010**. The Effect of "*Teucrium polium L.*" Extracts on insulin release from *in situ* isolated perfused rat pancreas in a newly modified isolation method: the role of Ca^{2+} and K^+ channels. Iran Biomed J, 14: 178-185.

Mithieux G, Rajas F, Gautier-Stein A, **2004**. A novel role for glucose 6-phosphatase in the small intestine in the control of glucose homeostasis. J Biol Chem, 279: 44231-44234.

Ohtsubo K, Chen MZ, Olefsky JM, Marth JD, **2011**. Pathway to diabetes through attenuation of pancreatic beta cell glycosylation and glucose transport. Nat Med, 17: 1067-1075.

Patel, K, Raj BS, Chen Y, Lou X, **2016**. Cytotoxicity of folic acid conjugated hollow silica nanoparticles toward Caco2 and 3T3 cells, with and without encapsulated DOX. Colloids Surf B, 140: 213-222.

Rorsman P, **Ashcroft** FM, **2018**. Pancreatic β-Cell Electrical Activity and Insulin Secretion: Of Mice and Men. Physiol Rev, 98(1): 117-214. doi: 10.1152/physrev.00008.2017. PMID: 29212789; PMCID: PMC5866358.

Rossetti L, Shulman G, Zawalich W, DeFronzo R, **1987**. Effect of chronic hyperglycemia on in vivo insulin secretion in partially pancreatectomized rats. J Clin Invest, 80: 1037-1044.

Ruas JS, Siqueira-Santos ES, Amigo I, Rodrigues-Silva E, Kowaltowski AJ, Castilho RF, **2016**. Underestimation of the maximal capacity of the mitochondrial electron transport system in oligomycin-treated cells. PloS One, 11(3): e0150967. PubMed PMID: 26950698; PubMed Central PMCID: PMC4780810.

Rutter GA, Pullen TJ, Hodson DJ, Martinez-Sanchez A, 2015. Pancreatic β-cell identity, glucose sensing and the control of insulin secretion. Biochem J, 466: 203-218.

Schuit FC, Huypens P, Heimberg H, Piperleers DG, **2001**. Glucose sensing in pancreatic -cells a model for the study of other glucose-regulated cells in gut, pancreas, and hypothalamus. Diabetes, 50(1): 1-11. https://doi.org/10.2337/diabetes.50.1.1

Sekine N, Cirulli V, Regazzi R, Brown LJ, Gine E, Tamarit-Rodriguez J, Girotti M, Marie M, MacDonald MJ, Wollheim, CB, **1994**. Low lactate dehydrogenase and high mitochondrial glycerol phosphate dehydrogenase in pancreatic beta-cells. Potential role in nutrient sensing. J Biol Chem, 269: 4895-4902.

Shahraki MR, Arab MR, Mirimokaddam E, Palan MJ, **2007**. The effect of Teucrium polium (Calpoureh) on liver function, serum lipids and glucose in diabetic male rats. Iran Biomed J, 11: 65-68.

Sharififar F, Dehghn-Nudeh G, Mirtajaldini M, 2009. Major flavonoids with antioxidant activity from *Teucrium polium* L. Food Chem, 112: 885-888.

Soares JMD, Perieira Leal AEB, Silva JC, Almeida JRGS, de Oliveira, HP, **2017**. Influence of Flavonoids on Mechanism of Modulation of Insulin Secretion. Pharmacogn Mag, 13: 639-646.

Stefkov G, Kulevanova S, Miova B, Dinevska-Kjovkarovska S, Mølgaard P, Jäger AK, Josefsen K, **2011**. Effects of Teucrium polium spp. capitatum flavonoids on the lipid and carbohydrate metabolism in rats. Pharm Biol, 49: 885-892.

Suckale J, **Solimena** M, **2008**. Pancreas islets in metabolic signaling-focus on the beta-cell. Front. Biosci, 13: 7156-7171.

Tal M, Liang Y, Najafi H, Lodish H, Matschinsky F, **1992**. Expression and function of GLUT-1 and GLUT-2 glucose transporter isoforms in cells of cultured rat pancreatic islets. J Biol Chem, 267: 17241-17247.

Tarasov A, Dusonchet J, Ashcroft F, **2004**. Metabolic regulation of the pancreatic beta-cell ATP-sensitive K+ channel. Diabetes, 53(Suppl 3): S113-S122

Vessal M, Zal F, Vaseei M, **2003**. Effects of *Teucrium polium* on oral glucose tolerance test, regeneration of pancreatic islets and activity of hepatic glucokinase in diabetic rats. Arch Iran Med, 6: 35-39.

WHO, **2006**. Definition and Diagnosis of Diabetes Mellitus and Intermediate Hyperglycaemia: Report of a WHO/IDF Consultation. [(accessed on 26 June 2022)]. Available online: https://www.who.int/publications/i/item/definition-and-diagnosis-of-diabetes-mellitus-and-intermediate-hyperglycaemia.